Chapter 8

Co-Evolution of Morphology and Mind

Morphology and materials are intimately related to control in adaptive behavior (Pfeifer 2000). This is referred to as ecological balance and was argued to enable better designs of robots and other artificial organisms. There is a trade-off between morphology and control: having the right morphology can greatly simplify controller requirements. As such, it was also argued that discussions of embodied autonomous agents pertaining only to neural processing issues are incomplete without a related discussion of the agent's shape, physical properties of its sensors and motors as well as the materials which make up the agent's body and appendages.

The term co-evolution as used in the field of evolutionary computation usually refers to the concurrent evolution of two or more populations with fitness functions that are coupled dynamically (Rosin and Belew 1997). These co-evolutionary algorithms can either consist of competing populations (Hillis 1992; Angeline and Pollack 1993; Cliff and Miller 1996; Rosin and Belew 1997; Nolfi and Floreano 2000; Floreano, Nolfi, and Mondada 2001) or cooperative populations (Husbands and Mill 1991; Paredis 1995; Potter and De Jong 2000). However, here we use the term co-evolution as previously used by Dellaert and Beer (1994), Lee, Hallam, and Lund (1996), and Hornby and Pollack (2001a) to refer to the simultaneous evolution of both morphology and controller in evolving artificial creatures rather than to refer

to competing or cooperating populations with coupled fitness functions.

In this chapter, we will attempt to evolve both the creature's morphology and mind. This will be achieved by relaxing certain morphological constraints imposed on the artificial creature where the focus thus far has only been on the optimization of its ANN controller. We will now include the parameters of the creature's ANN controller as well as morphology into the chromosome to allow for both aspects of the creature's body and mind to be optimized simultaneously through co-evolution. As we have seen from the literature survey conducted in Chapter 2, there are two extremes in evolving artificial creatures where on the one hand all of the morphology is totally fixed and unchangeable such as in the more common four-legged and six-legged physical robots, and on the other hand virtually all aspects of the morphology are changeable such as in abstract robots. Thus, we have adopted an approach midway between these extremes and evolve only certain parameters of the artificial creature's morphology and maintain some underlying body plan representative of quadrupedal organisms. The objective of this chapter is thus to explore not only the legged locomotion behavior that can be achieved by co-evolving both the morphology and controller but also the selective adaptation of body parts and joint constraints by evolution for efficient legged locomotion.

8.1 Additional Chromosome Parameters

To allow for the morphology of the creature to be simultaneously co-evolved with its ANN controller, we relax two specific aspects of the quadruped's morphology. The first constraint relaxed is the length of each of the upper and lower limbs in each of the four legs, which are now variable in length. The second constraint relaxed is the manner in which each limb is connected to the adjoining body part, where a choice of how the upper limb joins to the torso as well as how each lower limb joins to each upper limb is now available. These additional evolutionary parameters arising from the relaxation of the morphological constraints are added to the existing chromosome structure as previously explained in Section 3.4. More ex-

planation concerning the addition of these new genes into the chromosome is given in the following paragraphs.

Limb Description	Previous Length	New Length
Upper back left	1.0	$0.2 + (L1 \times 4.0)$
Upper front left	1.0	$0.2 + (L2 \times 4.0)$
Upper back right	1.0	$0.2 + (L3 \times 4.0)$
Upper front right	1.0	$0.2 + (L4 \times 4.0)$
Lower back left	1.0	$0.2 + (L5 \times 4.0)$
Lower front left	1.0	$0.2 + (L6 \times 4.0)$
Lower back right	1.0	$0.2 + (L7 \times 4.0)$
Lower front right	1.0	$0.2 + (L8 \times 4.0)$

Table 8.1: Description of the simulated quadruped's previous fixed limb lengths and new evolvable limb lengths (in centimeters).

Table 8.1 lists the artificial creature's previous and new limb lengths. Previously, the length of each limb was fixed to only 1cm. In the new design, each limb has a minimum length of 0.2cm and to that is added a length that can vary from 0 to 4cm. These variable attributes are denoted *L1* through *L8* and are included into the chromosome as continuous variables taking values between 0 and 1. As such, the dimensions of the limbs are now $1 \times 1 \times (0.2 + (L \times 4))$cm.

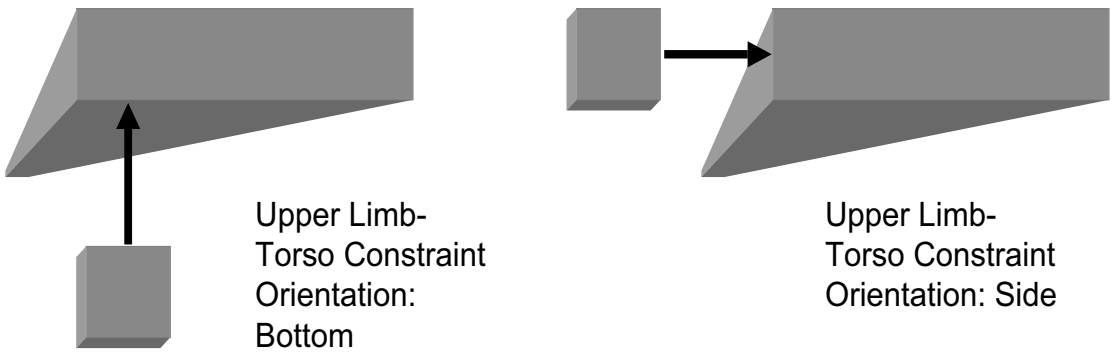

Figure 8.1: Front-on view of the evolvable constraint orientation for the joint connection between the torso and upper limbs 1. bottom-oriented connection (left), 2. side-oriented connection (right).

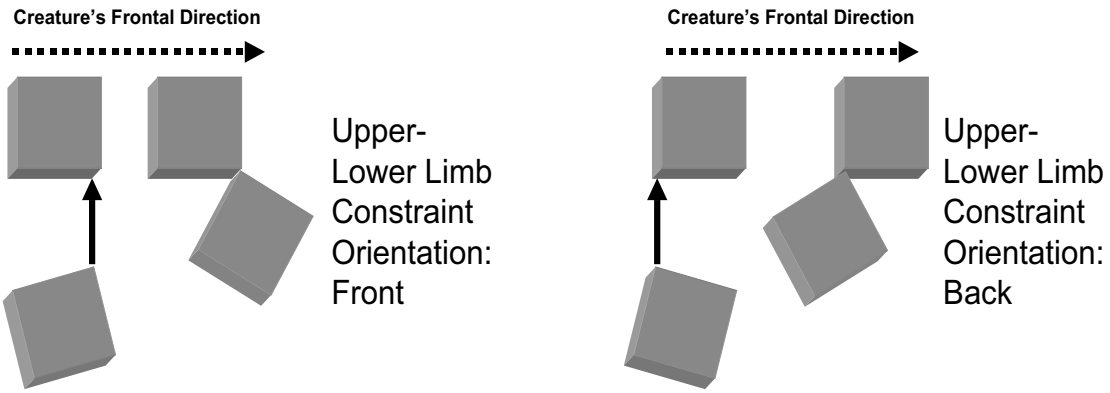

Figure 8.2: Side-on view of the evolvable constraint orientation for the joint connection between upper and lower limbs 1. front-oriented connection (left), 2. back-oriented connection (right).

Limb Description	**Connected To (Limb)**	**Previous Constraint Orientation**	**New Constraint Orientation**
Upper back left	Torso	Side	Side or Bottom (*C1*)
Upper front left	Torso	Side	Side or Bottom (*C2*)
Upper back right	Torso	Side	Side or Bottom (*C3*)
Upper front right	Torso	Side	Side or Bottom (*C4*)
Lower back left	Upper back left	Back	Back or Front (*C5*)
Lower front left	Upper front left	Back	Back or Front (*C6*)
Lower back right	Upper back right	Back	Back or Front (*C7*)
Lower front right	Upper front right	Back	Back or Front (*C8*)

Table 8.2: Description of the simulated quadruped's previous fixed constraint orientations and new evolvable constraint orientations.

Table 8.2 lists the artificial creature's previous and new limb constraint orientations. In the previous setup, all joint connections were fixed to either side or back orientations depending on whether it was an upper or lower limb. In the new setup, there is now a choice of constraint orientation for each of the eight joint connections. Each upper limb can now be connected to the torso either from side (Figure 8.1.1) or from the bottom (Figure 8.1.2). Each lower limb can now be connected to each upper limb either from the front (Figure 8.2.1) or from the back (Figure 8.2.2). These variable attributes are denoted *C1* through *C8* and are

included into the chromosome as Boolean variables that denote either one of the two orientation choices.

8.2 Experimental Setup

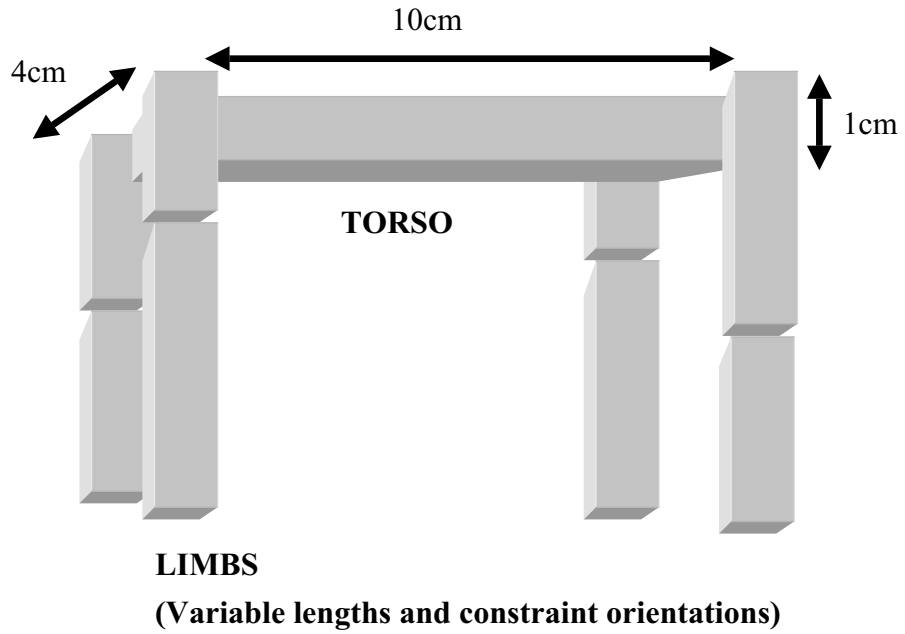

Figure 8.3: A geometric description of the new artificial creature used in the co-evolutionary experiments with evolvable limb lengths and evolvable constraint orientations. The torso dimensions are fixed as denoted.

A series of 10 independent runs were carried out to investigate the co-evolution of morphology and controller simultaneously. SPANN was used as the algorithm for driving the artificial evolutionary optimization process again. This augmented version which allows for the co-evolution of morphology and mind is denoted as the SPANN-CMM algorithm. A number of the artificial creature's setup was changed in SPANN-CMM to accommodate the additional evolvable components of its morphology. All changes were scaled linearly in relation to the original quadruped's setup discussed in Section 3.2. A geometric description of the new

artificial creature is given in Figure 8.3. The torso dimension was increased to $10 \times 4 \times 1$cm and the mass increased to 5g. From initial co-evolutionary experiments, the original shorter torso length of 4cm caused the limbs with longer lengths to constantly come in contact with each other during the locomotion cycle and thus restricted full movement of the limbs. Hence the length of the torso was increased to 10cm to allow for full and unhindered movement of the longer limbs. Furthermore, the creature frequently toppled over when longer limbs were present, therefore the width of the torso was also increased from 2cm to 4cm to allow for greater stability. As outlined in the introduction to this chapter, we wished to maintain some basic quadrupedal body plan and as such, we kept the torso fixed as a hand-designed component of the artificial creature and not part of the evolvable morphology. The mass of each limb and force generated at each associated hinge joint were also scaled linearly in accordance with the length of the associated limbs as they evolved. The maximum rotation allowed at each hinge joint remained unchanged at 1.57 radians. The ANN architecture used was NNType3 since it gave the best overall results from prior experiments. All other evolutionary and simulation parameters remained the same: 1000 generations, 30 individuals, 500 timesteps and a maximum of 15 hidden units allowed in the ANN controller.

In the analysis, we first discuss the best solutions obtained from the evolutionary runs using SPANN-CMM in terms of the locomotion behavior and size of the ANN controller as well as comparing the results against SPANN. This is followed by a simple characterization of the search space associated with this co-evolutionary setup. We then use the complexity measure defined in the previous chapter to conduct a simple comparison of the different creatures evolved with and without co-evolution of morphology.

8.3 Results and Discussion

Table 8.3 shows the best results obtained using SPANN-CMM in terms of locomotion distance. The overall best f_1 fitness was slightly better than SPANN

Algorithm	Overall Best f_1 Fitness	Worst of Best f_1 Fitness	Average Best f_1 Fitness ± Standard Deviation	t-statistic (against SPANN)
SPANN-CMM	18.1472	11.9002	15.1421 ± 2.0321	1.63
SPANN	17.6994	11.3234	13.9626 ± 1.7033	-

Table 8.3: Comparison of best locomotion distance for Pareto solutions found using the SPANN-CMM and SPANN algorithms over 10 independent runs.

achieving a locomotion distance of 18.1 units. The average locomotion distance of the best evolved controllers were also slightly higher than those obtained using SPANN although the improvement was not statistically significant.

Table 8.4 shows the best results obtained using SPANN-CMM in terms of number of hidden units used in the ANN controllers. The overall best f_2 fitness was slightly worse than SPANN using 1 more hidden unit. The worst of the best f_2 fitness was also slightly worse than SPANN using 2 more hidden units. The average number of hidden units used in the best evolved controllers was also slightly higher than those obtained using SPANN although the increase was not statistically significant.

Algorithm	Overall Best f_2 Fitness	Worst of Best f_2 Fitness	Average Best f_2 Fitness ± Standard Deviation	t-statistic (against SPANN)
SPANN-CMM	3	11	6.4 ± 2.8	1.15
SPANN	2	9	4.9 ± 2.6	-

Table 8.4: Comparison of smallest hidden layer size for Pareto solutions found using the SPANN-CMM and SPANN algorithms over 10 independent runs.

In general, the results in terms of the best solutions obtained at the end of co-evolving both the morphology and controller were not very different for both the locomotion distances achieved as well as number of hidden units used in the ANN controller.

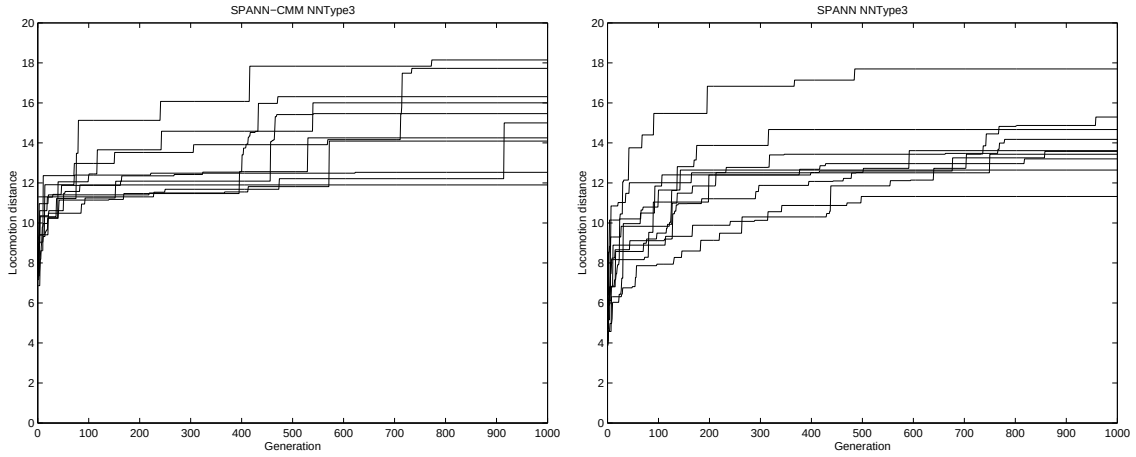

Figure 8.4: Comparison of best locomotion distance of Pareto solutions obtained over 1000 generations for 10 runs using the 1. SPANN-CMM (left), 2. SPANN (right) algorithms. X-axis: Generation, Y-axis: Locomotion distance.

8.3.1 Evolutionary Dynamics

Two interesting characteristics emerged in the evolutionary dynamics of the best solutions in SPANN-CMM (Figure 8.4.1). Firstly, although some significant improvements in the locomotion fitness were observed early during the evolutionary process, significant improvements still occurred during the later stages of evolution. In six of the runs, large improvements occurred between the 400–600th generation. One of these six runs later showed another large improvement around the 700th generation. Another separate run showed a large improvement as late as the 900th generation. Secondly, the improvements were very discrete in nature, some improving over 3 units of locomotion distance in a single generation. Both these characteristics were in contrast to those observed in SPANN where the majority of the improvements occurred well before the 200th generation and occurred much more gradually (Figure 8.4.2). This suggests firstly that evolution might have discovered a significantly better morphology during the co-evolutionary optimization process and hence a large improvement in locomotion distance could be achieved within a single generation. Secondly, SPANN-CMM may require more time to converge on a solution by virtue of the increased number of evolutionary parameters

resulting from the inclusion of additional morphological parameters into the chromosome. Thus, the solutions found may still be some distance away from the actual Pareto-frontier of optimal solutions. In order to test this second postulation, we extended the best run (the tenth seed), which still showed a noticeable improvement at the 773rd generation, beyond 1000 generations for another 500 generations from the 773rd generation but found no further improvements. Hence, the second postulation that the co-evolutionary runs require more time to converge is unlikely to be true since the best run had in fact converged to a final solution by the 1000th generation.

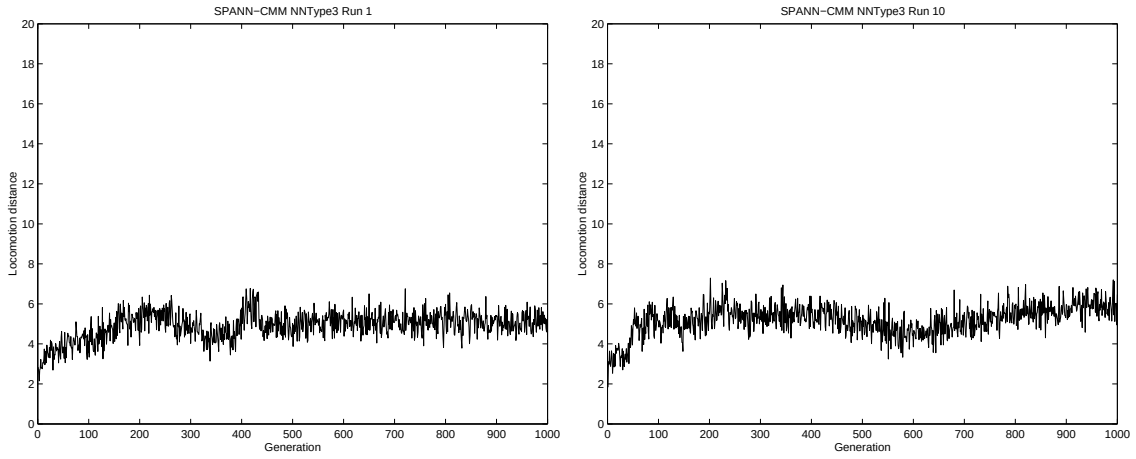

Figure 8.5: Mean locomotion distance of population over 1000 generations for the SPANN-CMM algorithm using the 1. first (left), 2. tenth (right) seeds. X-axis: Generation, Y-Axis: Locomotion distance. Additional graphs can be found in the accompanying CD-ROM.

The variation in SPANN-CMM's population mean tended to either remain fixed within a certain range or increase slightly over time, as illustrated by Figures 8.5.1 and 8.5.2 respectively. The standard deviation in the population was generally quite high, varying mostly between 3 and 4 in the earlier half of evolution then tending towards 5 in the later half of evolution, as shown by Figure 8.6.1, and even 6 in some of the runs, as shown by Figure 8.6.2. This is most probably due to the generation of new individuals which have morphologies that may not be easily

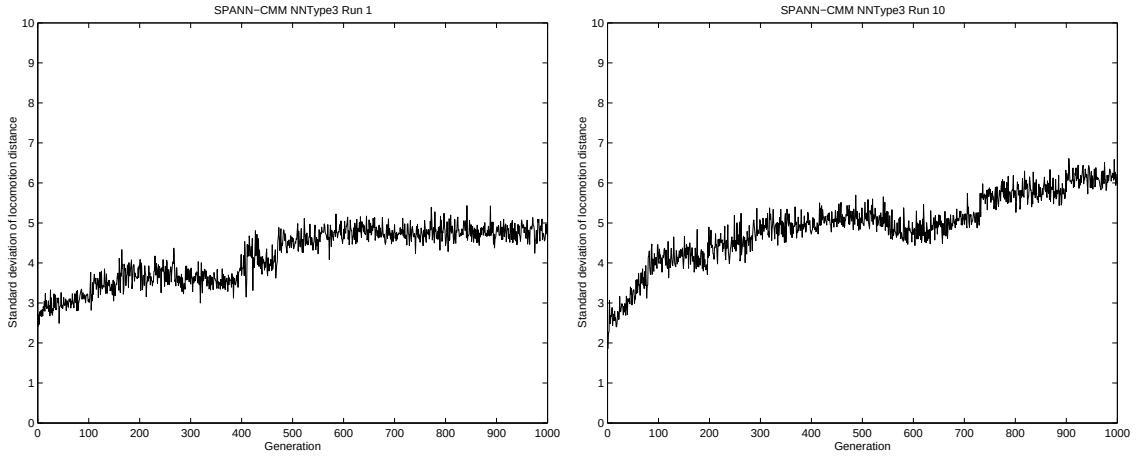

Figure 8.6: Standard deviation for locomotion distance of population over 1000 generations for the SPANN-CMM algorithm using the 1. first (left), 2. tenth (right) seeds. X-axis: Generation, Y-Axis: Standard deviation of locomotion distance. Additional graphs can be found in the accompanying CD-ROM.

controlled by the existing ANN controllers. Consequently, a larger gap will exist between the optimized solutions that have controllers and morphologies that work well together and the newly generated solutions that don't as evolution progresses.

8.3.2 Comparing Pareto-Fronts and Morphological Complexity

Table 8.5 lists the global Pareto solutions obtained using SPANN-CMM followed by those obtained using SPANN. The Pareto-front is highly similar to that obtained using SPANN although SPANN-CMM did have one more solution on the Pareto-front which used 6 hidden units and achieved the best locomotion distance. In general, the locomotion distances achieved with each hidden layer size was highly similar. No trend could be observed with the controllers that were comparable, with three hidden layer sizes achieving slightly higher locomotion distances in SPANN-CMM (networks using 1, 2 & 3 hidden units) and two hidden layer sizes performing slightly better in SPANN (networks using 0 & 4 hidden units).

Figure 8.7 compares the Pareto optimal solutions obtained using SPANN-

Algorithm	No. of Hidden Units	Locomotion Distance
SPANN-CMM	0	14.2775
	1	15.8432
	2	17.0130
	3	17.2338
	4	17.6614
	6	18.1472
SPANN	0	14.7730
	1	15.7506
	2	16.2295
	3	17.0663
	4	17.6994

Table 8.5: Comparison of number of hidden units and locomotion distance for global Pareto optimal controllers obtained using the SPANN-CMM and SPANN algorithms over 10 independent runs.

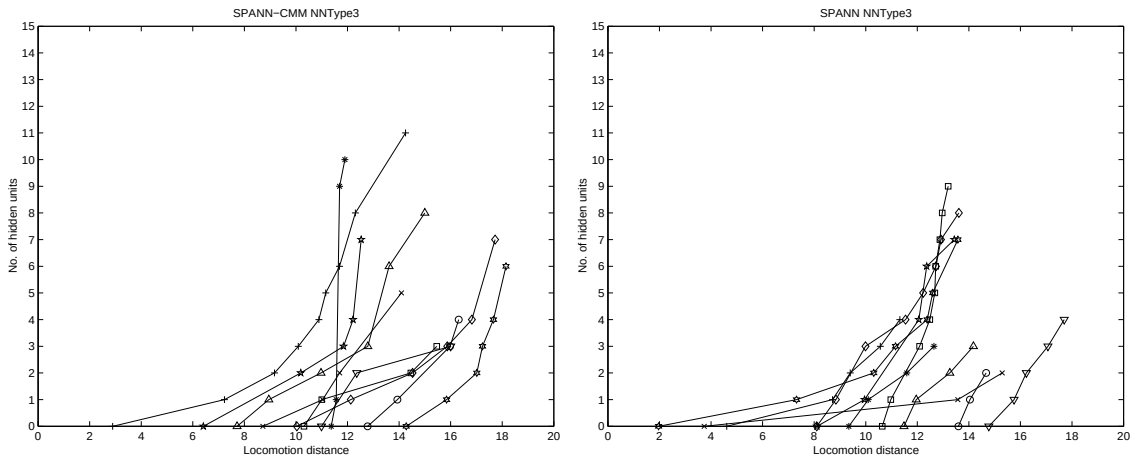

Figure 8.7: Pareto-front of solutions obtained for 10 runs using the 1. SPANN-CMM (left), 2. SPANN (right) algorithms. X-axis: Locomotion distance, Y-axis: No. of hidden units.

CMM against SPANN over 10 runs. As in Section 7.5.1, we are comparing two Pareto-fronts that characterize the complexities of two different morphologies. Here the environment E and learning algorithm L are again fixed, so we can either measure the change of morphological complexity in the eyes of the behavior or the controller: that is, $\frac{\partial f(B)}{\partial M}$ or $\frac{\partial f(C)}{\partial M}$ respectively. If we fix the actual behavior B as the locomotion competency of achieving a movement of $13 < d < 15$, then the change

in the controller $\partial f(C)$ is measured according to the number of hidden units used in the ANN. At this point of comparison, we find that both SPANN-CMM (Figure 8.7.1) and SPANN (Figure 8.7.2) produced creatures that were able to achieve the desired behavior with 0 hidden units. Therefore, this is an indication that from the controller's point of view, given the change in morphology ∂M from the creature evolved by co-evolving morphology and controller to the fixed morphology creature, there was no increase in complexity for the controller ∂C. Hence, the SPANN-CMM morphology can be seen as being at the same level of complexity as the SPANN morphology in the eyes of the controller.

Conversely, we can also measure the complexity of the morphology from the eyes of the locomotion behavior. First we need to choose a common point of comparison in terms of the network size. If we fix the controller C to having a hidden layer size of 3 hidden units, then the change in the locomotion behavior $\partial f(B)$ is measured according to the maximum distance achieved by artificial creatures. At this point of comparison, we find again that the creatures evolved with both SPANN-CMM (Figure 8.7.1) and SPANN (Figure 8.7.2) achieve a similar locomotion distance of 17 units. Thus, this is an indication that from the locomotion behavior's point of view, given the change in morphology ∂M from the co-evolved morphology and fixed morphology, there was no increase in complexity for the locomotion behavior ∂B. In this case, the SPANN-CMM morphology can again be seen as having the same level of complexity as the SPANN morphology.

Table 8.6 lists the evolved values for the variable parameters in the creature's morphology for the global Pareto solutions found by SPANN-CMM. The limb length values for Pareto solutions 2 through 5 were very similar while solutions 1 and 6 were slightly more different. In Pareto solutions 2 through 5, the only difference in limb length was found in gene *L5* of 0.1cm. Pareto solution 1 had a longer limb length for genes *L5* and *L6* while Pareto solution 6 had a longer limb length for gene *L4* compared to the other Pareto solutions. There was more variation in terms of the constraint orientation found in the Pareto solutions although some common choices of orientation could still be found. All *C1*, *C5* and *C8* genes had similar

Pareto Solution No.	1	2	3	4	5	6
Locomotion Distance	14.3	15.8	17.0	17.2	17.7	18.1
No. of Hidden Units	0	1	2	3	4	6
L1	0.2	0.2	0.2	0.2	0.2	0.2
L2	0.2	0.2	0.2	0.2	0.2	0.2
L3	4.1	4.1	4.1	4.1	4.1	4.1
L4	0.2	0.2	0.2	0.2	0.2	3.8
L5	4.0	2.7	2.8	2.7	2.8	2.8
L6	3.8	0.2	0.2	0.2	0.2	0.2
L7	0.6	0.6	0.6	0.6	0.6	0.2
L8	0.2	0.2	0.2	0.2	0.2	0.2
C1	side	side	side	side	side	side
C2	bottom	bottom	bottom	side	bottom	side
C3	side	side	side	side	side	bottom
C4	side	bottom	bottom	side	side	side
C5	back	back	back	back	back	back
C6	back	back	back	back	front	back
C7	back	front	front	back	front	back
C8	front	front	front	front	front	front

Table 8.6: Evolved limb lengths and constraint orientations for global Pareto optimal controllers obtained using the SPANN-CMM algorithm. Numerical values are rounded to 1 decimal place in this table.

values while C3 and C6 genes were similar in five out of the six Pareto solutions. It is very hard to generalize on why the evolutionary runs have converged on the limb length and constraint orientation gene values. Although it may be likely that longer limb lengths provided an evolutionary advantage in that artificial creatures with longer limbs should be able to move further distances per cycle of limb, not all of the solutions had maximal limb lengths. In fact, a number of limbs had the minimal value of 0.2cm such as *L1*, *L2* and *L8*. This combination of very small limb lengths actually resulted in entire legs that did not contribute to the locomotion of the creature upon visual inspection. This is somewhat analogous to vestigial limbs found in some animals. The presence of the non-contributing limbs may have lead to easier control requirements for the creature's legged locomotion. Screen dumps of the creature for the six global Pareto solutions are given below to provide a visualization of the evolved morphologies and the locomotion behavior generated.

Visual inspection of the locomotion behavior generated by the creatures

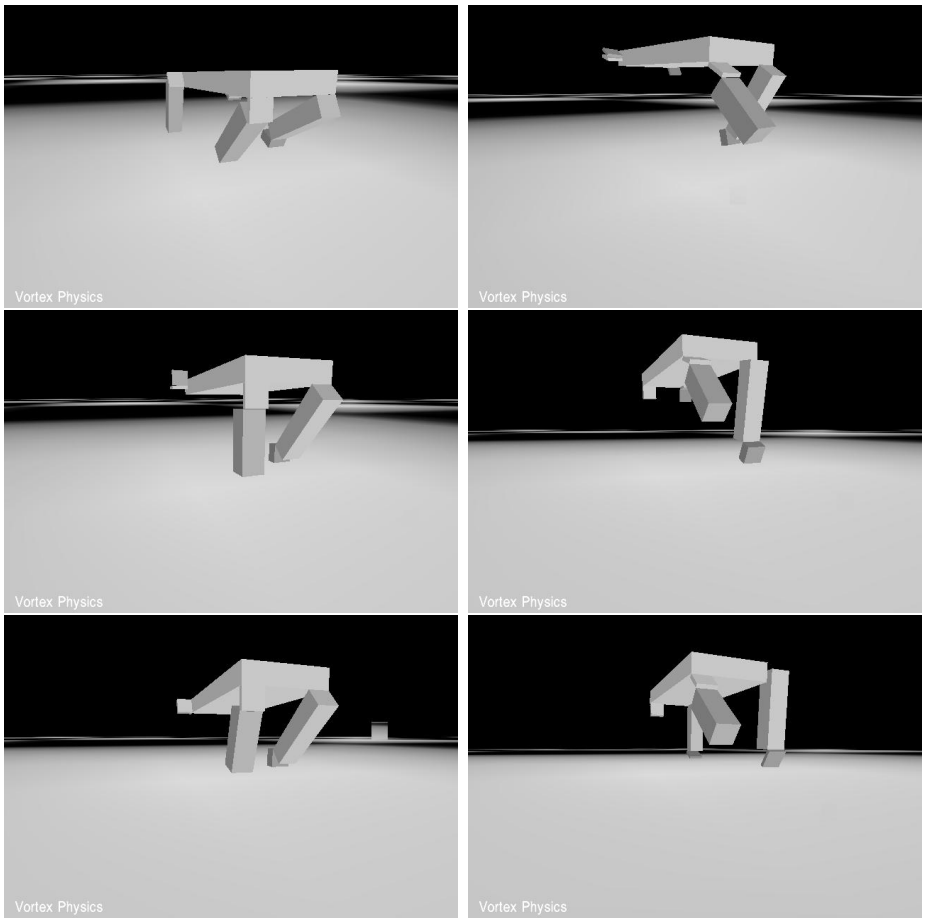

Figure 8.8: Screen dumps of the artificial creatures found on the global Pareto-frontier from co-evolving morphology and controller. 1. Solution 1 (top left), 2. Solution 2 (top right), 3. Solution 3 (middle left), 4. Solution 4 (middle right), 5. Solution 5 (bottom left), 6. Solution 6 (bottom right).

found on the global Pareto-frontier of the evolutionary runs revealed that all the creatures moved forwards by using a dynamic jumping gait rather than a statically stable walking gait (interested readers can view video clips of these evolved behaviors in the accompanying CD-ROM). Creature 1 (Figure 8.8.1) was basically a tripedal creature which generated its locomotion force from its front left, back right and back left legs while having a non-contributing front right leg. Creatures 2 through 5 (Figures 8.8.2–8.8.5) were essentially bipedal creatures that had almost identical morphologies and resultant gaits, where the locomotion force was generated by the two back legs while the two front limbs did not contribute to the forwards move-

ment. Creature 6 (Figure 8.8.6) again returned to the tripedal-like morphology seen in Creature 1. However the non-contributing leg was now switched to the front left and the locomotion force was generated by the front right, back right and back left legs. Across all the creatures, it is interesting to note that the legs which contributed to the forwards locomotion had fairly similar overall leg lengths although the individual limbs that made up the overall leg were quite different between the upper and lower limbs. Furthermore, the non-contributing limbs were fully minimized to the shortest possible length. As postulated earlier, this may somehow simplify the control requirements of the creature by reducing the number of legs that actually touched the ground during the creature's movement and hence did not require any synchronization within these legs nor coordination with other contributing legs to occur.

8.3.3 Search Space Characteristics

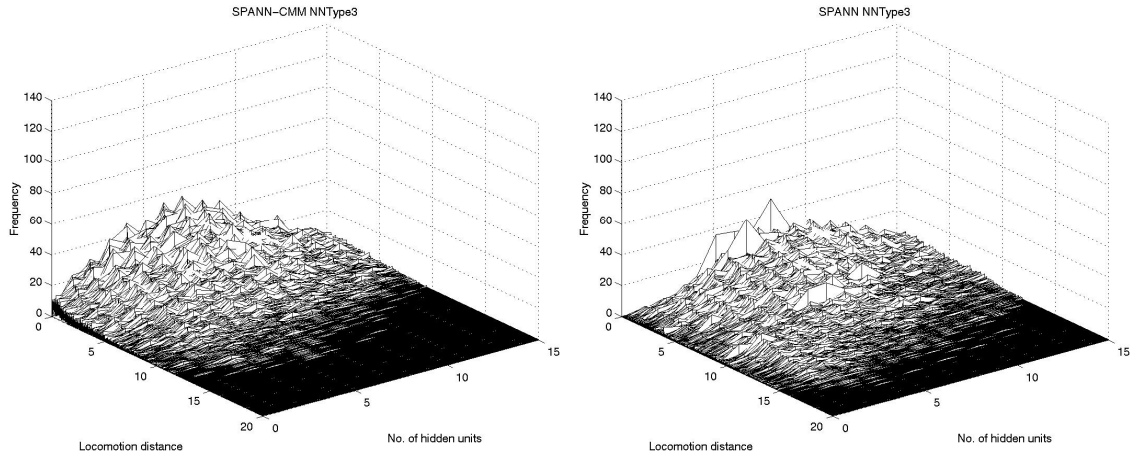

Figure 8.9: Frequency distribution of solutions obtained using the 1. SPANN-CMM (left), 2. SPANN (right) algorithms. X-axis: Locomotion distance, Y-axis: No. of hidden units, Z-axis: Frequency.

The frequency distribution of genotypes generated by SPANN-CMM across the two objective spaces were fairly uniformly spread out as depicted in Figure 8.9.1, similar to the frequency distribution obtained for SPANN (Figure 8.9.2). The

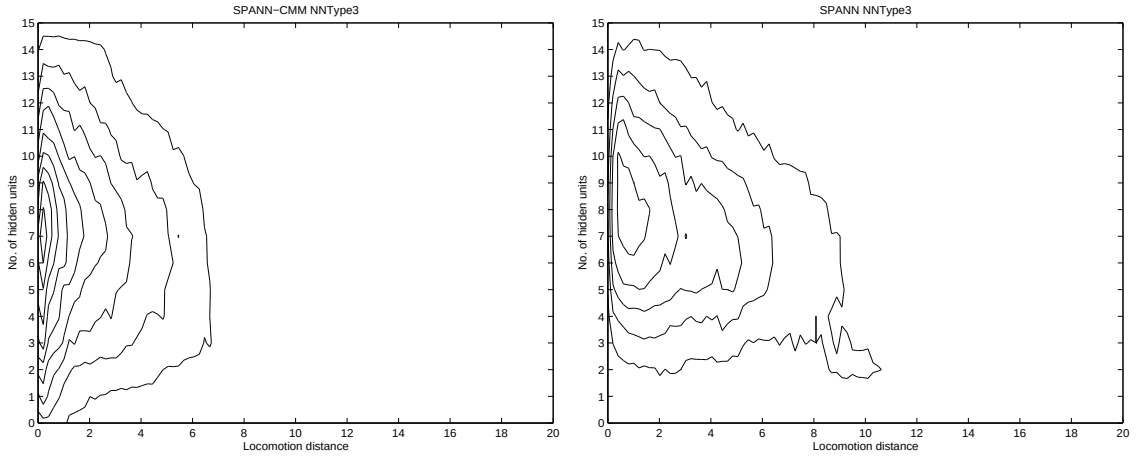

Figure 8.10: Contour graphs of frequency distribution of solutions obtained using the 1. SPANN-CMM (left), 2. SPANN (right) algorithms. X-axis: Locomotion distance, Y-axis: No. of hidden units.

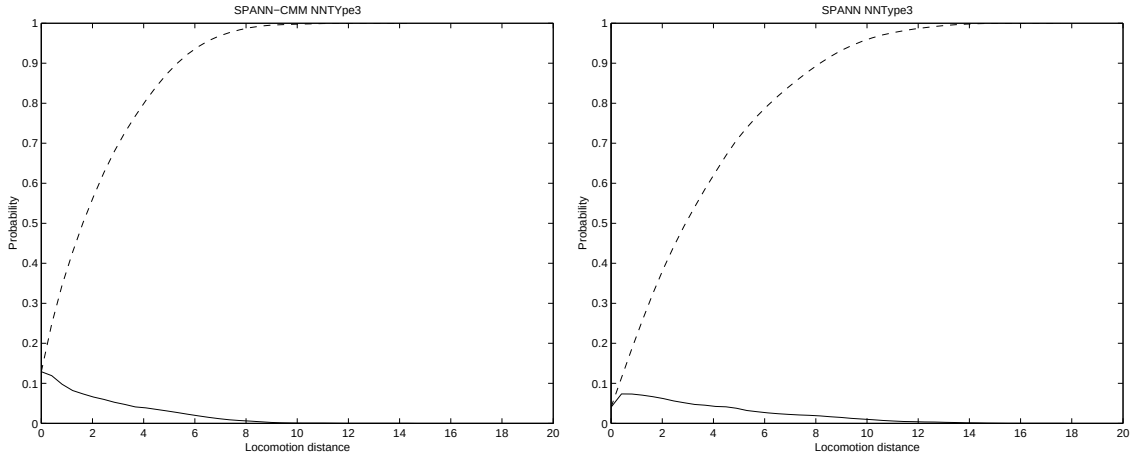

Figure 8.11: Density (solid) and cumulative (dashed) probability distribution of solutions obtained using the 1. SPANN-CMM (left), 2. SPANN (right) algorithms. X-axis: Locomotion distance, Y-axis: Probability.

contour graph in Figure 8.10.1 shows that the highest concentration of genotypes generated by SPANN-CMM used between 6 and 8 hidden units in the controller and produced very bad locomotion capabilities. Again, this can be attributed to the changing morphology of the creature, of which some may be very hard to generate good locomotion behaviors by virtue of their physical characteristics. From the

contour graphs, it can be seen that the distribution of solutions in terms of the two objectives were more spread out and less clustered within a specific region in SPANN (Figure 8.10.2) compared to SPANN-CMM, and as such was able to sample areas of the search space with higher locomotion fitness. The probability density function for SPANN-CMM shows that the probability of encountering solutions dropped to zero at around 12 units of distance (Figure 8.11.1) compared to SPANN which extended to around 14 units (Figure 8.11.2). However, the fact that SPANN-CMM was still able to produce controllers with locomotion distances higher than SPANN in spite of having a higher concentration of solutions in the lower fitness regions of the objective space shows that the inclusion of morphological parameters for evolution is not entirely counterproductive but can in fact find good combinations of controller and morphology.

8.4 Chapter Summary

We have investigated the co-evolution of morphology and mind by augmenting the SPANN algorithm to allow for simultaneous optimization of both the creature's body and controller. Certain morphological parameters which were previously constrained have been relaxed to allow for the ANN controller to be optimized while at the same time allowing evolution to find suitable morphologies that would work well with the controllers. It was found that although no significant improvement in locomotion distance was achieved, significantly different locomotion behaviors emerged together with radically different body designs. Dynamic locomotion gaits based on a jumping motion generated mainly from hind legs were found in creatures that were essentially bipedal and tripedal in their legged locomotion. A characterization of the different solutions showed that the creatures existing on the global Pareto-frontier had similar complexities in terms of both control and locomotion behavior.